Available online at www.sciencedirect.com
ScienceDirect
Polymer 48 (2007) 1903–1914
polymer
www.elsevier.com/locate/polymer

Magnetic field effects on the free radical solution polymerization of acrylamide

Ignacio Rintoul, Christine Wandrey*

Ecole Polytechnique Fédérale de Lausanne (EPFL), Institut de Bioingénierie, Station 15, CH-1015 Lausanne, Switzerland

Received 24 September 2006; received in revised form 1 February 2007; accepted 2 February 2007
Available online 7 February 2007

Abstract

Systematic polymerization experiments quantified magnetic field (MF) influences on the free radical solution polymerization of acrylamide for various polymerization conditions. The type of initiation, the initiator concentration, the monomer concentration, and the viscosity of the aqueous medium were the subject of variation. The initiator efficiency (Φ) increased up to 60% and the initiator exponent of the overall rate expression raised from 0.1 to 0.28 when a weak MF of 0.1 T was applied to photochemical initiation. However, no appropriate effect was observed for thermal initiation. Kinetic analysis proved a reduction of the termination rate coefficient (k_t) up to 40%. Photochemically initiated polymerizations in media of enhanced viscosity revealed the highest increment of the initiator efficiency ratio Φ^{MF}/Φ and the most pronounced reduction of k_t^{MF}/k_t. On the contrary, the propagation rate coefficient (k_p) and the monomer exponent were not influenced by MF. Despite considerable increase of the polymerization rate in MF, no reduction of the molar mass was found. Compensation of increased Φ^{MF} and decreased k_t^{MF} are suggested as explanation. The singlet–triplet intersystem crossing mechanism for radical pairs served to explain the MF effects.

Keywords: Free radical polymerization; Magnetic field; Acrylamide

1. Introduction

Magnetic field (MF) effects are potentially of technological interest. The MF interacts with matter in a relatively homogenous manner, can excite molecules selectively, and has the ability to control the course and the rate of reactions, which, normally, requires much higher activation energies [1]. Magnetic effects on the polymerization of acrylonitrile [2,3], styrene [4], methyl methacrylate [4–6], and butyl methacrylate [4,7] have been investigated under various conditions. In general, the application of MF was found to increase the rate of polymerization (R_p), conversion, homogeneity, and molar mass of the products. Moreover, MF effects were most pronounced for polymerizations carried out in viscous polar media. In particular, the solution photopolymerization of acrylamide (AM) in binary mixtures of water/ethylene glycol (EG) has shown increased R_p [8]. Similar results were obtained for the photopolymerization of AM in water and water/methanol mixtures [6]. Though for the latter solvent mixture, lower polymer yield and higher molar mass were reported under MF.

Overall, MF effects are explained in terms of the radical pair mechanism [9]. Radical pairs are generated in singlet (S) or triplet (T_+, T_0, T_-) spin states from precursors having their respective multiplicity, or else, when formed by free radical encounters. These spin states describe different electron configurations. Depending on these configurations the radical pair will undergo several reactions: recombination, which regenerates the initial molecule, formation of cage products, which generates a new molecule, or the radicals can escape from the cage and release two free radicals to the reaction medium. Fig. 1a shows a vector representation of the spin states. When the electrons are immersed in a MF of intensity B_0 and arbitrary z-direction, the energy of the states (the Zeeman

* Corresponding author. Tel.: +41 21 693 96 61; fax: +41 21 693 96 85.
E-mail address: christine.wandrey@epfl.ch (C. Wandrey).

0032-3861/$ - see front matter © 2007 Elsevier Ltd. All rights reserved.
doi:10.1016/j.polymer.2007.02.002

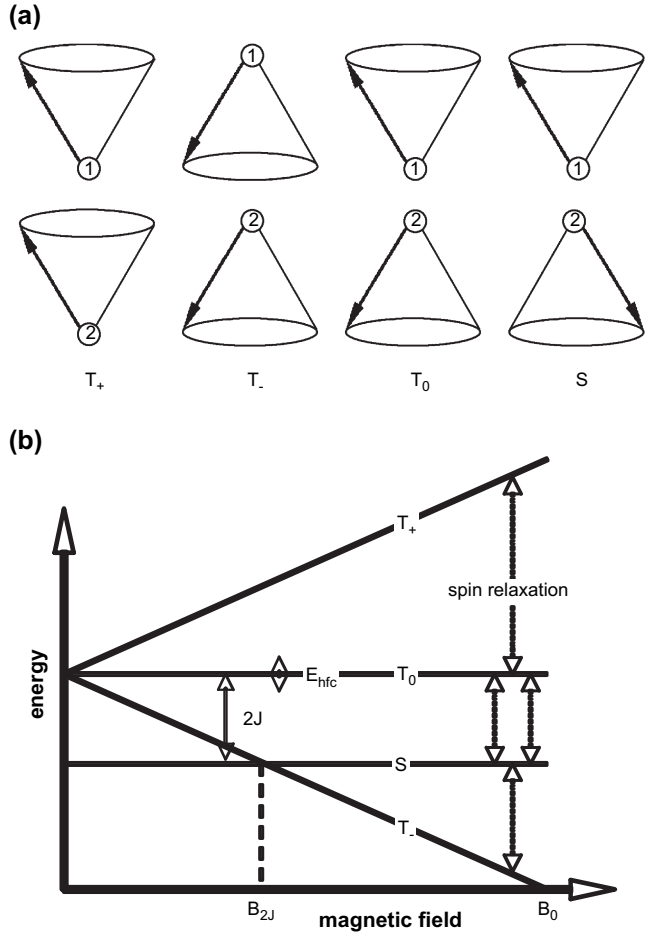

Fig. 1. (a) Vector representation of the singlet and triplet spin states. (b) Zeeman energy levels of spin states as a function of the magnetic field. E_{hfc} is the average bandwidth due to hyperfine coupling and J is the energy associated with T–S transitions (adapted from Ref. [9]).

energy levels) may be expressed as: $E = g\beta B_0 \sum S_z$. Here g and β are the dimensionless electron g factor ($g = 2.002322$) and the Bohr magneton ($\beta = 0.92731\ 10^{-20}$ erg/gauss), respectively. The sum is over all electronic spin contributions in the direction of the MF, S_z. Only two unpaired electrons are involved in a radical pair. Each has a quantized contribution ($S_z = +1/2$ or $S_z = -1/2$) in the direction of the field. Then, the Zeeman energy associated with the pure S, T_+, T_-, and T_0 electronic spin states is: $E_S = 0$, $E_{T_+} = g\beta B_0$, $E_{T_-} = -g\beta B_0$, and $E_{T_0} = 0$. It is obvious that the energy associated with the T_+ and T_- increases and decreases proportionally with B_0, while the energy of the S and T_0 states is unaffected by the MF. It is important to mention that the T_0 state presents a non-zero component in a direction perpendicular to B_0, while the S state results zero in all directions, i.e. it is a real basic state. Fig. 1b schematizes the Zeeman energy levels as a function of MF.

Radical pairs in S state have extremely high probability to undergo recombination reactions. On the contrary, radical pairs in any of the three T states cannot recombine. Nevertheless, radicals may pass from one state to another through intersystem crossing mechanisms [9]. The application of MF splits out the Zeeman energy levels of the T states diminishing substantially the probability for intersystem crossing to the S state. Therefore, primary radical pairs can be quenched in T state decreasing the probability of radical recombination. Consequently, more radicals are released to the polymerization medium resulting in an increase of the initiator efficiency leading to an increase of R_p. Furthermore, when two growing radicals encounter each other in the T state, they cannot recombine. Thus, they continue growing while increasing the molar mass of the final products. Additionally, MF is able to orient molecules in the polymerizing medium, which can, indeed, accelerate the polymerization and can be favorable for the quality of the reaction products.

The literature about MF effects on polymerization reactions is abundant. A number of mechanisms have been established and received proper theoretical treatment. Nevertheless, the majority of publications focuses on comparative studies. In general, the correlation between classical chemical reaction parameters and MF effects is missing. In fact, the topic was recently evaluated as deserving further studies [10]. As to the authors' knowledge, the influence of the MF on the rate coefficients of initiation, propagation, and termination has not been investigated in detail for the free radical polymerization of acrylamide.

The goal of this investigation is to analyze the extent of MF effects on the kinetics of initiation, propagation and termination of free radical photopolymerization, and to conclude consequences for the overall rate expression (Eq. (1) [11]), as well as for the molar mass of the products. A mechanistic discussion of the interaction between MF and reactants will be included.

$$R_p = -\frac{d[M]}{dt} = k_p[M]^{\alpha}\left(\frac{\Phi\varepsilon I_0[I]}{k_t}\right)^{\beta} \quad (1)$$

R_p is the polymerization rate defined as the negative derivative of the monomer concentration with time. $[M]^{\alpha}$ and $[I]^{\beta}$ are the monomer and initiator concentrations in mol/l powered to their respective reaction order α and β. k_p and k_t are the propagation and termination rate coefficients (l/mol s). Φ is the initiator efficiency. ε is the molar absorptivity (l/mol cm) of the photoinitiator. I_0 is the light intensity in moles of light quanta per liter and second (mol/l s).

The polymerization of AM in solution, photochemically initiated with phenyl-bis(2,4,6-trimethylbenzoyl)-phosphine oxide, $C_{26}H_{27}O_3P$, was investigated under various conditions with and without the influence of MF. The photochemical decomposition of $C_{26}H_{27}O_3P$ is well known [12]. Initially, $C_{26}H_{27}O_3P$ undergoes a photoinduced cleavage of the carbonyl–phosphinoyl (C–P) bond yielding a benzoyl and a phosphinoyl primary radical pair in triplet spin state trapped in a cage, which is formed by solvent and monomer molecules. Once created, the radicals can separate into two free radicals, which are able to add the first monomer molecule and initiate a polymer chain, or they can undergo recombination, regenerating $C_{26}H_{27}O_3P$, which is again able to form a radical pair. Though, the radical can also produce a variety of cage products, which are unable to yield radicals. The parameter that considers all

these reactions is Φ, defined here as the portion of radical pairs that successfully initiate polymerization steps per light quantum absorbed.

The C–P cleavage of $C_{26}H_{27}O_3P$ molecules depends on ε and I_0. ε was reported as 8170 l/mol cm [13] and 7931 l/mol cm [14] . As to the authors' knowledge, no data are reported for β in the case of $C_{26}H_{27}O_3P$. However, significant deviations from the ideal value 0.5 were reported for several other photoinitiators: $\beta = 0.21$ for pyridinium chlorochromate [15], 0.27 for 2,2-dimethoxy-2-phenylacetophenone [16] and *tert*-butylcyclohexyl-peroxydicarbonate [17], and 0.30 for triphenyl-bismuthonium-1,2,3,4-tetraphenyl-cyclopentadienylide [18]. In general, primary radical termination was suggested as the reason for such low initiator exponent values.

The polymerization of AM has intensely been studied [19–31]. Nevertheless, the propagation mechanism is still debated. The values of α, k_p and k_t were reported to be influenced by pH [19–21], temperature [22], and solvent type [23] due to the ionization of the monomer and growing radicals [19,20], the formation of dimers and H-bonds [21,22,25], changes in the conformation of growing radicals [21], and the formation of monomer–initiator complexes prior to the initiator decomposition [24].

Based on conclusions from published data, the experimental conditions of this study were selected in such a way that side effects related to pH, temperature, and solvents are minimized or even avoided. These prerequisites were met by preparing aqueous monomer solutions at pH ≈ 4 [21] and polymerizing in a temperature range of 312–322 K [22]. pH ≈ 4 ensures electrochemical neutrality of AM and growing radicals [21]. Polymerizing at $313 < T < 323$ K let expect the absence of H-bond effects [22]. Thus, exclusively information about the MF effects and related mechanisms should become significant. Under such conditions, $8.11 \times 10^4 < k_p < 10.38 \times 10^4$ l/mol s for [AM] = 0.32 mol/l [25], and k_t in the order of 3.3×10^6 l/mol s [20] were reported. Moreover, several authors published α values only slightly different from unity: 1.00 [26,27], 1.04 [28], 1.07 [29], 1.10 [30], and 1.16 [31]. Various amounts of EG were mixed with water to vary the viscosity of the reaction medium but maintaining good solvation properties for the reactants and the reaction products [8].

The only parameters in Eq. (1), which can definitely be assumed as independent of MF, are [M], [I], and I_0. [M] and [I] are given by the recipe of the batch. I_0 is a characteristic of the UV lamp. It only depends on the geometry of the reactor. All other parameters need evaluation.

2. Experimental section

2.1. Materials

White crystals of ultra pure AM, 4 times recrystallized (AppliChem – Axon Lab AG, Switzerland), were selected as monomer. An aqueous dispersion of phenyl-bis(2,4,6-trimethylbenzoyl)-phosphine oxide, $C_{26}H_{27}O_3P$ (Ciba Specialty Chemicals, Switzerland) and potassium persulfate, $K_2S_2O_8$ (Fluka Chemie, Switzerland) served as photoinitiator and thermal initiator. The water was of Millipore quality (18.2 MΩ/cm). Ethylene glycol 99% for synthesis (EG) was used to vary the viscosity of the polymerization medium. HPLC grade acetonitrile (AppliChem – Axon Lab AG, Switzerland) served to precipitate the polymer in the withdrawn samples.

2.2. Polymerization conditions

Syntheses were performed in a 100 ml glass reactor, which was designed and manufactured for the polymerization study herein (3 cm diameter, 15 cm height). It was equipped with a UV lamp, stirrer, condenser, gas inlet, and a heating/cooling jacket. The UV lamp had a primary output at 254 nm wavelength with an intensity $I_{UV} = 540$ erg/s cm^2 at the surface of the lamp (45 cm^2). I_{UV} was considered as constant and uniform everywhere in the reaction medium due to the dimension of the reactor. It was recalculated into I_0, the parameter needed for Eq. (1); $I_0 = 5.16 \times 10^{-8}$ mol/l s was obtained. The reactor was entirely placed between the poles of a 2 T electromagnet (Bruker-EPRM, Germany). A thermostat was used to adjust the reaction temperature to be within ±1 K. Oxygen was removed from the initial monomer solution by purging with N_2 ($O_2 < 2$ ppm; Airliquide, Switzerland) for 30 min at room temperature (293 K) and 0 T of MF intensity. After degassing, the temperature was raised, and the UV lamp was lighted to activate the photodecomposition of $C_{26}H_{27}O_3P$. Simultaneously, the MF was adjusted to 0.1 T. Complementary experiments were carried out without MF, though keeping constant all the other conditions.

All reactions were performed isothermally during 60 min purging continuously with N_2 and irradiating the reactor with the UV light. Samples of 0.1–0.2 g were withdrawn from the reactor every 5 min for kinetic analysis. Table 1 summarizes the conditions of all polymerizations. First, an initiator-free aqueous AM solution was illuminated with UV light for 1 h at 313 K (series 1) to prove the absence of monomer photolysis, which could generate radicals disturbing the polymerization path. Another AM solution containing $C_{26}H_{27}O_3P$ was maintained in darkness for 1 h at 323 K (series 2) to demonstrate the absence of thermal decomposition of the photoinitiator. Series 3 and 4 were AM polymerizations using $K_2S_2O_8$ and $C_{26}H_{27}O_3P$ as thermal and photoinitiators. These series were intended to obtain information about the MF effects on

Table 1
Experimental conditions of AM polymerizations, $T = 313$ K, MF = 0.1 T

Series	[AM] (mol/l)	[Initiator] (mol/l)	EG (wt%)	MF[b]
1	0.2	0	50	–
2[a]	0.2	$[C_{26}H_{27}O_3P] = 1 \times 10^{-5}$	50	–
3	0.2	$[K_2S_2O_8] = 1.12 \times 10^{-2}$	50	–/+
4	0.2	$1.5 \times 10^{-6} < [C_{26}H_{27}O_3P] < 1 \times 10^{-5}$	0	–/+
5	0.2	$[C_{26}H_{27}O_3P] = 1 \times 10^{-6}$	$0 < EG < 80$	–/+
6	$0.025 < [AM] < 0.150$	$[C_{26}H_{27}O_3P] = 1 \times 10^{-5}$	80	–/+
7	0.5	$[C_{26}H_{27}O_3P] = 1 \times 10^{-6}$	80	–/+

[a] $T = 323$ K.
[b] Without MF, –; with MF, +.

the propagation step and on the initiator exponent in the overall rate expression. Further, AM was polymerized in aqueous solutions with different contents of EG (series 5) and at different monomer concentrations (series 6) to study the influence of viscosity and monomer concentration on the extent of MF effects. Finally, photopolymerizations of AM were performed up to different conversions (series 7) to see if there are MF effects on the molar mass of the resulting polymers. Series 3–7 were performed with and without MF at 313 K.

2.3. Conversion analysis and polymerization rate

The conversion was determined by analyzing the residual monomer concentration. It served to calculate R_p according to a recently reported procedure [32]. Briefly, the residual monomer concentration in the samples was monitored using an HPLC system composed of an L-7110 Merck–Hitachi pump (Hitachi, Japan) and a SP6 Gynkotek UV detector (Gynkotek, Germany) operating at $\lambda = 197$ nm. The stationary and mobile phases were LiChrosphere 100 RP-18 (Merck, Germany) and aqueous solutions containing 5 wt% acetonitrile. The flow rate was 1 ml/min. The HPLC system was calibrated using AM solutions of known concentrations. The concentration as a function of the peak area served as calibration parameter ($r^2 > 0.999$). The samples withdrawn from the reactor were mixed with 4 ml of acetonitrile to precipitate and isolate the polymer from the solution. The non-reacted monomers remained in the solution. Supernatant of 20 μl was injected for HPLC analysis.

2.4. Determination of the molar absorptivity of $C_{26}H_{27}O_3P$

The molar absorptivity of $C_{26}H_{27}O_3P$ was determined directly by measuring the absorbance in a spectrophotometer, and indirectly by kinetic analysis. The direct method permitted to obtain a reference value of ε under non-magnetic conditions. The direct method was not applicable under magnetic conditions. The reference value was subsequently used to validate the indirect method, which was carried out under magnetic and non-magnetic conditions.

The absorbance of aqueous $C_{26}H_{27}O_3P$ solutions with concentrations ranging from 1×10^{-6} to 6×10^{-5} mol/l was measured at $\lambda = 254$ nm in order to obtain ε. A UV/vis spectrophotometer Lambda 18 (Perkin–Elmer, USA) equipped with quartz cells of 1 cm optical path length was used. The absorbance values were plotted as a function of the $[C_{26}H_{27}O_3P]$ according to Beer's law: $A = \varepsilon l c$. Here A is the absorbance, l is the optical path length, and c is the concentration of the substance in solution. Although this method permitted to obtain ε with high precision, it was not appropriate for measurements under MF. Thus, a modified dead-end polymerization technique [33–35], based on Eq. (2), was used to calculate ε from kinetic data. The technique refers to a polymerization where the initiator concentration decreases to such a low value that the half-life of the propagating polymer molecules approximates that of the initiator. Under such conditions, polymerizations show limiting conversion of monomer to polymer at infinite reaction time.

$$-\frac{2}{I_0}\ln\left(1-\frac{\ln(1-P)}{\ln(1-P_\infty)}\right) = \varepsilon t \tag{2}$$

P and P_∞ are the conversions at actual (experimental) and infinite (extrapolated) times. ε is obtained from the slope, when the left side of Eq. (2) is plotted vs. the reaction time, t.

2.5. Calculation of the initiator efficiency

The kinetic chain length, ν, is the average number of monomer molecules consumed per radical that initiates a polymer chain. It can be expressed as the ratio of the propagation to the termination rate. This holds for steady state conditions in the absence of transfer reactions. The adaptation to the general photopolymerization case and further rearrangement yield the ratio $k_p/k_t^{0.5}$ as a function of ν, Φ, ε, I_0, [I], and [M]:

$$\frac{k_p}{k_t^{0.5}} = \frac{\nu(\Phi\varepsilon I_0[\mathrm{I}])^{0.5}}{[\mathrm{M}]} \tag{3}$$

Replacing the ratio $k_p/k_t^{0.5}$ in Eq. (1) by the right side term of Eq. (3), and suggesting $\alpha = 1$, $\beta = 0.5$, and that the initiator concentration decreases exponentially with time according to: $[\mathrm{I}] = [\mathrm{I}]_0 e^{-0.5\varepsilon I_0 t}$, yields:

$$-\frac{d[\mathrm{M}]}{dt} = \nu\Phi\varepsilon I_0[\mathrm{I}]_0 e^{-0.5\varepsilon I_0 t} \tag{4}$$

Integrating Eq. (4) between $t_0 = 0$ and the actual reaction time, t, and rearranging leads to:

$$\Phi = \frac{[\mathrm{M}]_0 - [\mathrm{M}]}{2\nu[\mathrm{I}]_0(1 - e^{-0.5\varepsilon I_0 t})} \tag{5}$$

Eq. (5) permits to obtain Φ as a function of the reaction time, if [M], ε, and ν are known.

Eqs. (3) and (5) give $k_p/k_t^{0.5}$ and Φ at any time or conversion of the polymerization. Here, the kinetic analysis was restricted to the initial state of the polymerization, i.e. the determination of ν, Φ, and $k_p/k_t^{0.5}$ at conversions <10%.

2.6. Determination of the kinetic chain length and macromolecular characterization

The kinetic chain length ν was calculated according to

$$\nu = \frac{M_n}{2m_0} \tag{6}$$

where M_n is the number-average molar mass, and m_0 is the molar mass of the monomer. In Eq. (6) it was assumed that propagating radicals terminate by combination. M_n was calculated using the relationship $[\eta] = 6.6 \times 10^{-3} M_n^{0.82}$ (ml/g). The relationship, which was obtained by membrane osmometry, is valid for water as solvent and $T = 303$ K [36].

The intrinsic viscosity, [η], was measured using an automatic capillary viscometer (Viscologic TI.1, SEMAtech, France) with a capillary of 0.58 mm diameter. M_n and ν were calculated from [η] values of polymers withdrawn at conversions <10%. In addition, dilution viscometry was used to characterize polymers withdrawn at higher conversion from polymerizations without and with MF (series 7) in order to identify the MF influence on macromolecular characteristics.

Polymer samples, withdrawn from the reactor, were precipitated in acetonitrile. The precipitates were removed from the solution by centrifugation at 8000 rpm for 20 min. The polymer was redissolved in water and again precipitated in acetonitrile and separated by centrifugation. Finally, the polymers were dried and, subsequently, aqueous polymer stock solutions of 1 mg/g were prepared for dilution viscometry.

2.7. Viscosity of the polymerization medium

EG/water mixtures were prepared, which contained weight fractions of EG from 0 to 1 and, additionally, 0.2 mol/l of AM. The dynamic viscosity, η, of the mixtures was measured at 313 K using a disc viscometer (Brookfield, USA) equipped with a disc spindle of 20 mm diameter rotating at 50 rpm. Each mixture was measured 5 times. Deviations were within 4%. Fig. 2 presents the average viscosity values as a function of the mixture composition.

2.8. Electromagnet calibration

The MF intensity was adjusted by varying the electrical current running through the bobbins of a 2 T electromagnet. Fig. 3 shows the MF intensity as a function of the electrical current.

All MF polymerizations were carried out at 0.1 T. This value was selected in order to minimize the MF fluctuations during the stabilization time, which was required to adjust a constant MF. MF fluctuations and stabilization periods increased with MF intensity. Such effects are the consequence of the magnetic inertia of the iron core of the magnet and the limitation of the power supply to reach instantaneously a high and stable electrical current through the bobbins of the magnet.

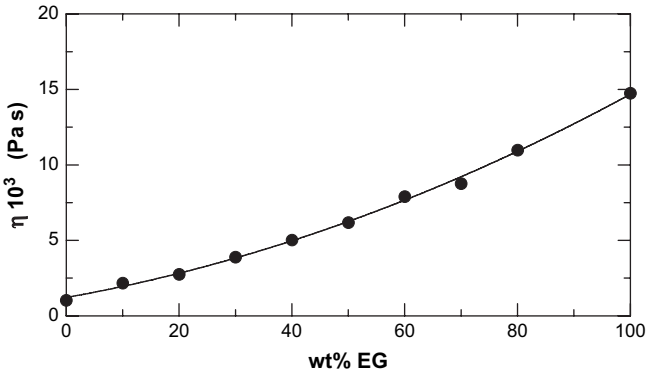

Fig. 2. Dynamic viscosity (η) of the polymerization medium as a function of the EG content in water, [AM] = 0.2 mol/l, T = 313 K.

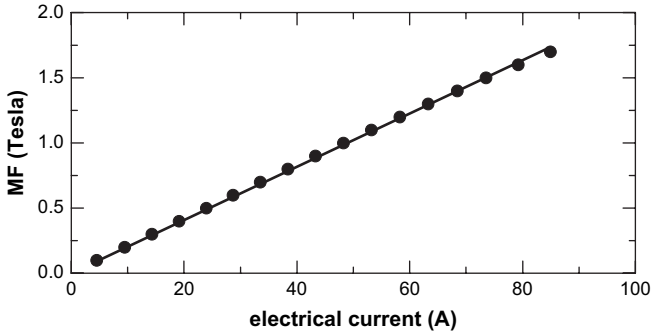

Fig. 3. Magnetic field (MF) strength vs. electrical current, $r^2 > 0.999$.

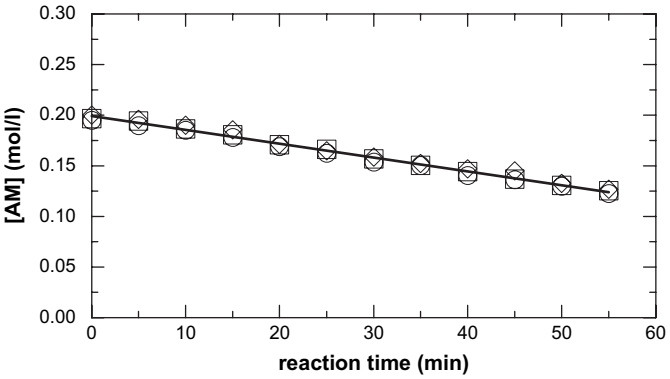

Fig. 4. Experimental reproducibility. AM polymerizations (○,□,◇) under identical conditions but with separately prepared batches and stock solutions, [AM] = 0.2 mol/l, $[K_2S_2O_8] = 3.2 \times 10^{-3}$ mol/l, T = 313 K.

2.9. Experimental accuracy and reproducibility

To evaluate the experimental accuracy a number of error sources were evaluated. A polymerization procedure, using $K_2S_2O_8$ as initiator at 313 K, was repeated 3 times. Fig. 4 presents the residual monomer concentration vs. reaction time.

The analysis of the residual monomer concentration [32] can be affected by the following error sources: the preparation of AM stock solutions, filling the reactor, withdrawing of samples, addition of acetonitrile, dilution of the supernatant, and injection in the HPLC system. Considering all error sources, the relative errors of the residual monomer concentration values were determined to be less than 6%. The R_p values differed by less than 3%.

3. Results

3.1. Evaluation of side effects and proof of MF effects

The absence of any polymerization was confirmed for series 1 and 2. On the contrary, AM polymerized when thermally (series 3) or photochemically (series 4–7) initiated. On the one hand, identical polymerization paths were obtained for

the thermally initiated AM polymerizations carried out with and without MF (series 3). On the other hand, a significant increment in R_p and P_∞ was observed for photopolymerizations carried out in the presence of MF. Fig. 5 visualizes the differences between thermally and photochemically initiated polymerizations carried out with and without MF.

3.2. Variation of the initiator concentration

Fig. 6 presents R_p and P_∞ as a function of $[C_{26}H_{27}O_3P]$ with and without MF, and using water as solvent. Here the superscript MF indicates that the value was obtained under the influence of MF. No clearly detectable MF effect was observed on R_p and P_∞ for $[C_{26}H_{27}O_3P] < 2 \times 10^{-6}$ mol/l. At such low initiator concentration retardation by residual oxygen becomes evident. The MF effect is visible for $[C_{26}H_{27}O_3P] > 2 \times 10^{-6}$ mol/l. The difference between R_p^{MF} and R_p approached 2.4×10^{-5} mol/l s corresponding to about 40% at $[C_{26}H_{27}O_3P] = 1 \times 10^{-5}$ mol/l. Higher differences in R_p may be concluded for higher $[C_{26}H_{27}O_3P]$. Though leveling off cannot be excluded. Unfortunately, polymerizations carried out at $[C_{26}H_{27}O_3P] > 1 \times 10^{-5}$ mol/l revealed a very short linear conversion period, preventing the accurate R_p determination. The slopes of the linear parts at $[C_{26}H_{27}O_3P] > 2 \times 10^{-6}$ mol/l in Fig. 6 were calculated as $\beta^{MF} = 0.28$ and $\beta = 0.10$ for polymerizations carried out with and without MF. These values correspond to the initiator exponent in Eq. (1). P_∞^{MF} was about 10% higher than P_∞ at $[C_{26}H_{27}O_3P] = 2 \times 10^{-6}$ mol/l. The difference diminishes with $[C_{26}H_{27}O_3P]$, finally approaching conversions >95%.

3.3. Variation of the viscosity

Fig. 7 shows how the viscosity of the polymerization medium and the MF affected R_p and P_∞. R_p^{MF} and R_p increased exponentially ($r^2 > 0.99$) when η was altered from 1.03×10^{-3} Pa s (aqueous AM solution) to 11.00×10^{-3} Pa s (80 wt% EG). The difference between R_p^{MF} and R_p (5.25×10^{-5} mol/l s) approached about 60% at the higher viscosity. The P_∞ values increased with R_p and η. The MF influence was not clearly detectable in the lower viscosity range. $P_\infty^{MF} > P_\infty$ was evident only for $\eta > 2 \times 10^{-3}$ Pa s. However,

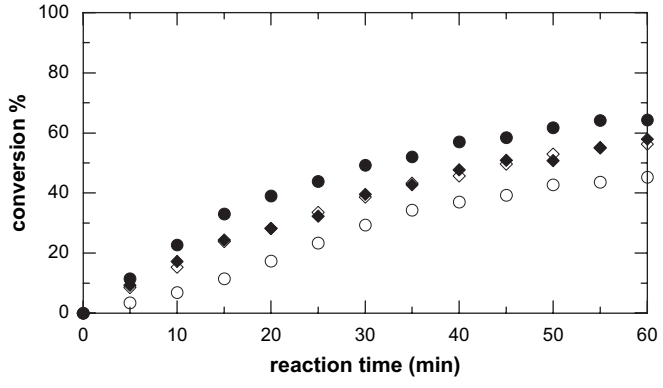

Fig. 5. Conversion curves of thermally (◆,◇) and photochemically (●,○) initiated polymerizations of AM carried out at 0.1 T (full symbols) and without MF (empty symbols). Thermal polymerizations: [AM] = 0.2 mol/l, $[K_2S_2O_8] = 1.12 \times 10^{-2}$ mol/l, $T = 313$ K. Photopolymerizations: [AM] = 0.2 mol/l, $[C_{26}H_{27}O_3P] = 1 \times 10^{-6}$ mol/l, $T = 313$ K. Solvent: 50 wt% EG in water.

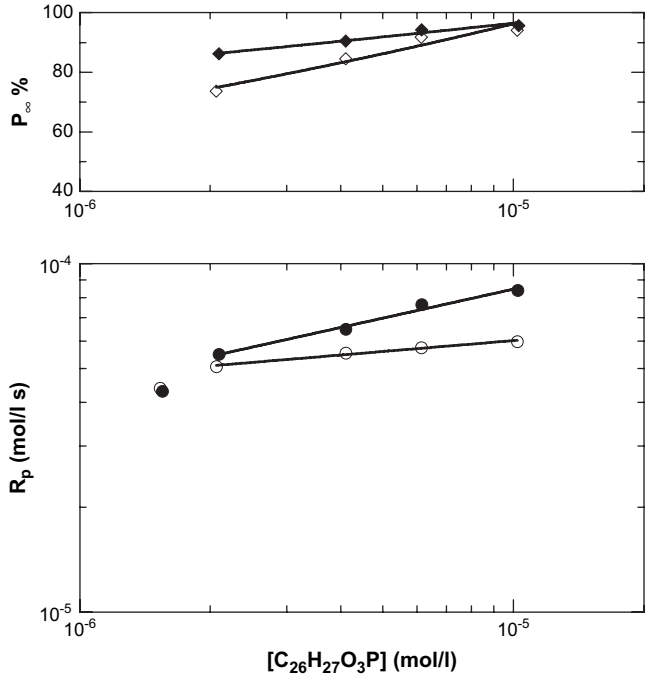

Fig. 6. Polymerization rate, R_p (●,○), and limiting conversion, P_∞ (◆,◇), for polymerizations carried out with (full symbols) and without (empty symbols) MF as function of $[C_{26}H_{27}O_3P]$. [AM] = 0.2 mol/l, $T = 313$ K, MF = 0.1 T, solvent: water.

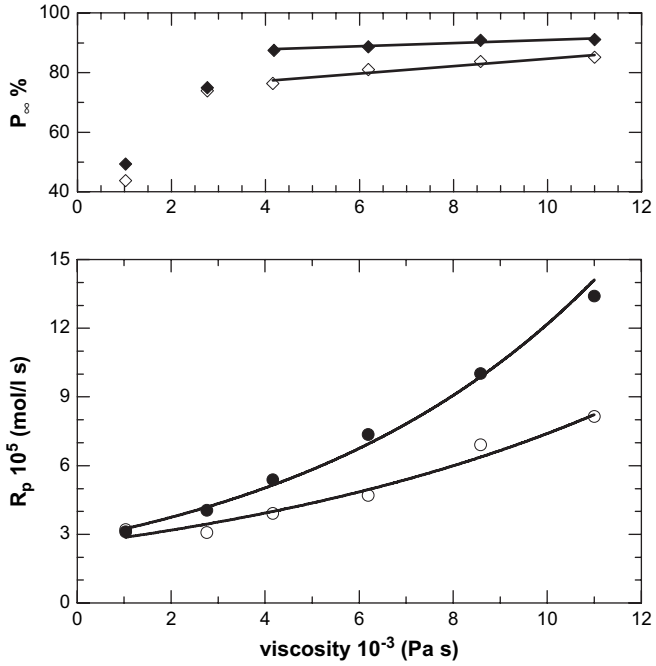

Fig. 7. Polymerization rate, R_p (●,○), and limiting conversion, P_∞ (◆,◇), for polymerizations carried out with (full symbols) and without (empty symbols) MF as function of the viscosity of the polymerization medium. [AM] = 0.2 mol/l, $[C_{26}H_{27}O_3P] = 1 \times 10^{-6}$ mol/l, $T = 313$ K, MF = 0.1 T.

it seems that P_∞^{MF} and P_∞ coincide at higher η. The dependencies were fitted as $R_p^{MF} = 2.79e^{0.149\eta}$ and $R_p = 2.58e^{0.106\eta}$. $[C_{26}H_{27}O_3P]$ was deliberately low (1×10^{-6} mol/l). This is in the range where no MF influence was observed due to the initiator concentration (see Fig. 6). This condition was selected to avoid the overlay of viscosity and initiator effects.

3.4. Variation of the monomer concentration

In Fig. 8, R_p and P_∞ of polymerizations in solutions with 80 wt% EG and $[C_{26}H_{27}O_3P] = 1 \times 10^{-5}$ mol/l are plotted as a function of [AM]. The conditions correspond to the most pronounced differences between R_p and R_p^{MF}, which were demonstrated in Sections 3.2 and 3.3. Both experimental series, with and without MF, presented linear ($r^2 > 0.99$) increments of R_p, while P_∞ approached constancy when [AM] was increased from 0.025 to 0.15 mol/l and $[C_{26}H_{27}O_3P]$ was 1×10^{-5} mol/l. Only minor or no influence of MF on P_∞ can be concluded from these experiments. R_p^{MF} resulted 1.65 times higher than R_p. The monomer exponent for Eq. (1) was obtained as $\alpha^{MF} = 1.12$ and $\alpha = 1.01$. Extrapolating to

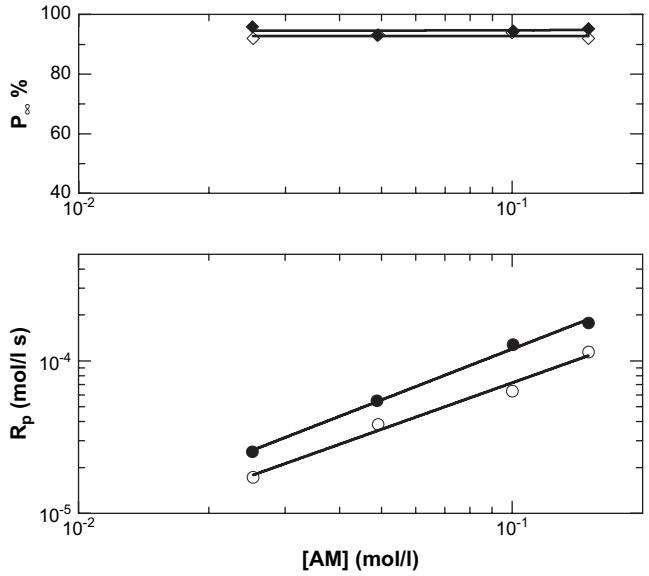

Fig. 8. Polymerization rate, R_p (●,○), and limiting conversion, P_∞ (◆,◇), for polymerizations carried out with (full symbols) and without (empty symbols) MF as function of [AM]. $[C_{26}H_{27}O_3P] = 1 \times 10^{-5}$ mol/l, $T = 313$ K, MF = 0.1 T. Solvent: 80 wt% EG in water.

$[AM] = 0.2$ mol/l yields a R_p difference of 1.1×10^{-4} mol/l s. This value is higher than reported for this initiator concentration and viscosity separately. It demonstrates the additivity of the initiator and viscosity effects, which were determined before separately in Sections 3.2 and 3.3.

3.5. Macromolecular characteristics

Table 2 summarizes $[\eta]$ as a function of the conversion as well as M_n and ν calculated thereof [36]. As expected, $[\eta]$ decreases with the conversion. However, it seems that $[\eta]$ was not affected by MF, as it is visualized in Fig. 9.

One has to be aware that the calculated M_n values are estimates not considering polydispersity and averaging influences. Nevertheless, the procedure is suited to evaluate tendencies and to identify differences. Moreover, since the type of the molar mass distribution primarily results from the termination mechanism and transfer side reactions, it can be assumed as not being affected by the MF. Therefore, the comparison of $[\eta]$ obtained for samples, which were polymerized without and with MF, at the same conversion is justified. Nevertheless, only ν for the initial state of the polymerizations was used for kinetic analysis.

3.6. Molar absorptivity of $C_{26}H_{27}O_3P$

Fig. 10 shows the absorbance of aqueous $C_{26}H_{27}O_3P$ solutions as a function of the concentration. $\varepsilon = 6700$ l/mol cm was obtained from the slope of the linear regression according to Beer's law.

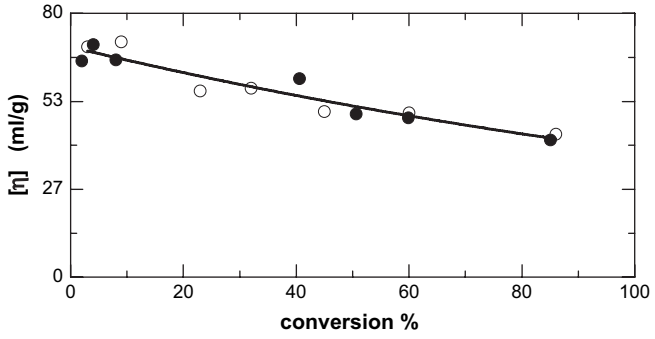

Fig. 9. Intrinsic viscosity of polyacrylamide synthesized with (●) and without (○) MF vs. conversions. [AM] = 0.5 mol/l, $[C_{26}H_{27}O_3P] = 1 \times 10^{-6}$ mol/l, $T = 313$ K, MF = 0.1 T, solvent: 80 wt% EG in water.

Table 2
Summary of characterization results (intrinsic viscosity $[\eta]$, number-average molar mass M_n, and kinetic chain length ν) obtained for polymers of series 7 in Table 1

No	Without MF					With MF = 0.1 T				
	Time (min)	Conv. (%)	$[\eta]$ (ml/g)	$M_n \times 10^{-4}$ (g/mol)	ν	Time (min)	Conv. (%)	$[\eta]$ (ml/g)	$M_n \times 10^{-4}$ (g/mol)	ν
7.1	1	3	69.9	11.4	800	0.25	2	65.6	10.5	740
7.2	2	9	71.4	11.7	821	0.50	4	70.6	11.5	811
7.3	5	23	56.5			1.00	8	66.0	10.6	745
7.4	7	32	57.3			3.00	41	60.3		
7.5	10	45	50.3			5.00	50	49.5		
7.6	15	60	49.9			7.00	60	48.4		
7.7	20	86	43.4			10.00	85	41.7		

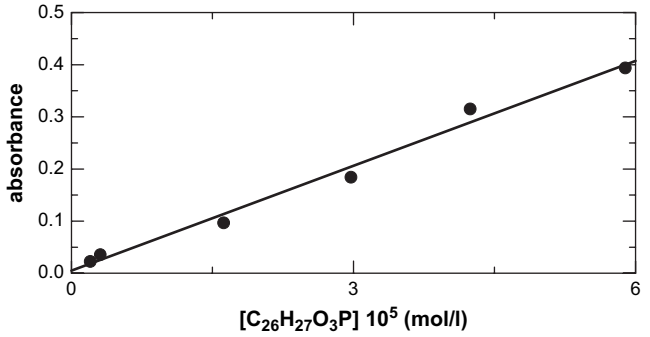

Fig. 10. Experimental determination of the molar absorptivity, ε, of $C_{26}H_{27}O_3P$ at $\lambda = 254$ nm, $r^2 > 0.98$.

Fig. 11 presents, exemplary, dead-end plots according to Eq. (2). The slopes of the linear regressions yielded ε. It is visible that the slopes remained constant within the experimental error when [AM] was modified in the range from 0.025 to 0.15 mol/l and during the 60 min of reaction time. Such constancy reveals that changes of [AM] and conversion did not alter ε under MF. The intercept increased with [AM] due to increasing R_p with the monomer concentration. Table 3 summarizes the ε values.

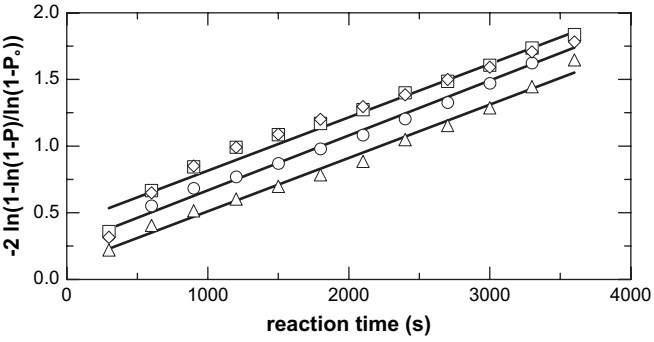

Fig. 11. Dead-end plots of series 6, [AM] = 0.025 (△), 0.05 (○), 0.1 (□), and 0.15 (◇) mol/l, $[C_{26}H_{27}O_3P] = 1 \times 10^{-5}$ mol/l, $T = 313$ K, solvent: 80 wt% EG in water, MF = 0.1 T.

The calculated ε values seem not to be affected by any of the experimentally varied conditions such as MF, $[C_{26}H_{27}O_3P]$, [AM], η, conversion, and reaction time. The experimental value from absorbance measurements is within the standard deviation of the values calculated using the procedure of Eq. (2), which yielded the average $\varepsilon = 7914 \pm 1260$ l/mol cm. The high standard deviation primarily results from the low accuracy of the P_∞ determination. Nevertheless, this value is more similar to the values 8170 and 7931 l/mol cm reported in Refs. [13] and [14], respectively.

3.7. Kinetic parameters and ratios

The initiator efficiency and the ratio $k_p/k_t^{0.5}$ were calculated inserting the experimental results of series 4–6, which were reported in Sections 3.2–3.5, in Eqs. (3) and (5). Table 3 summarizes all values.

Analyzing the calculated data reveals that Φ considerably increases with η, [AM], and MF, but decreases with $[C_{26}H_{27}O_3P]$. The MF effect on Φ is more evident at high monomer concentration and in solutions with high EG content, both with increments of 70% and 64%, respectively.

The variation of $[C_{26}H_{27}O_3P]$ from 1.53×10^{-6} to 10.21×10^{-6} mol/l increased the $k_p/k_t^{0.5}$ ratio about 35% when MF was applied, whereas the initiator concentration effect is not clear without MF. The augmentation of η from 1.028×10^{-3} to 11.0×10^{-3} Pa s increased $k_p/k_t^{0.5}$ by about 44% and 52%, without and with MF, respectively. The augmentation of [AM] from 0.025 to 0.15 mol/l decreased $k_p/k_t^{0.5}$ by a factor of about 2.3 without and with MF. In general, the application of MF increased the $k_p/k_t^{0.5}$ ratio above a certain threshold for the initiator concentration and the viscosity/EG content.

Table 3
ε, Φ, and $k_p/k_t^{0.5}$ as a function of $[C_{26}H_{27}O_3P]$, η, and [AM] for polymerizations with and without MF. MF = 0.1 T, $T = 313$ K

Conditions	Variable	MF = 0			MF = 0.1 T		
Series 4	$[C_{26}H_{27}O_3P] \times 10^6$ (mol/l)	$\varepsilon \times 10^{-3}$ (l/mol cm)	Φ	$k_p/k_t^{0.5}$	$\varepsilon \times 10^{-3}$ (l/mol cm)	Φ	$k_p/k_t^{0.5}$
4.3	1.53	6.94	0.18	21	9.09	0.19	20
4.4	2.06	7.50	0.15	23	6.40	0.18	22
4.5	4.11	6.83	0.09	23	6.83	0.11	24
4.6	6.13	7.70	0.06	24	7.06	0.09	26
4.7	10.21	7.35	0.04	23	7.14	0.06	27
Series 5	$\eta \times 10^3$ (Pa s)						
5.1	1.028	7.16	0.19	18	7.54	0.20	17
5.2	2.76	8.42	0.20	17	9.75	0.26	19
5.3	4.16	7.85	0.24	20	9.91	0.37	21
5.4	6.19	6.79	0.31	21	9.99	0.52	25
5.5	8.58	7.21	0.48	25	10.41	0.75	28
5.6	11.00	10.20	0.58	26	9.91	0.95	33
Series 6	[AM] (mol/l)						
6.1	0.025	7.56	0.06	44	6.53	0.09	52
6.2	0.050	7.58	0.14	32	7.56	0.21	38
6.3	0.100	7.35	0.22	21	7.12	0.51	28
6.4	0.150	9.31	0.40	19	6.44	0.68	22

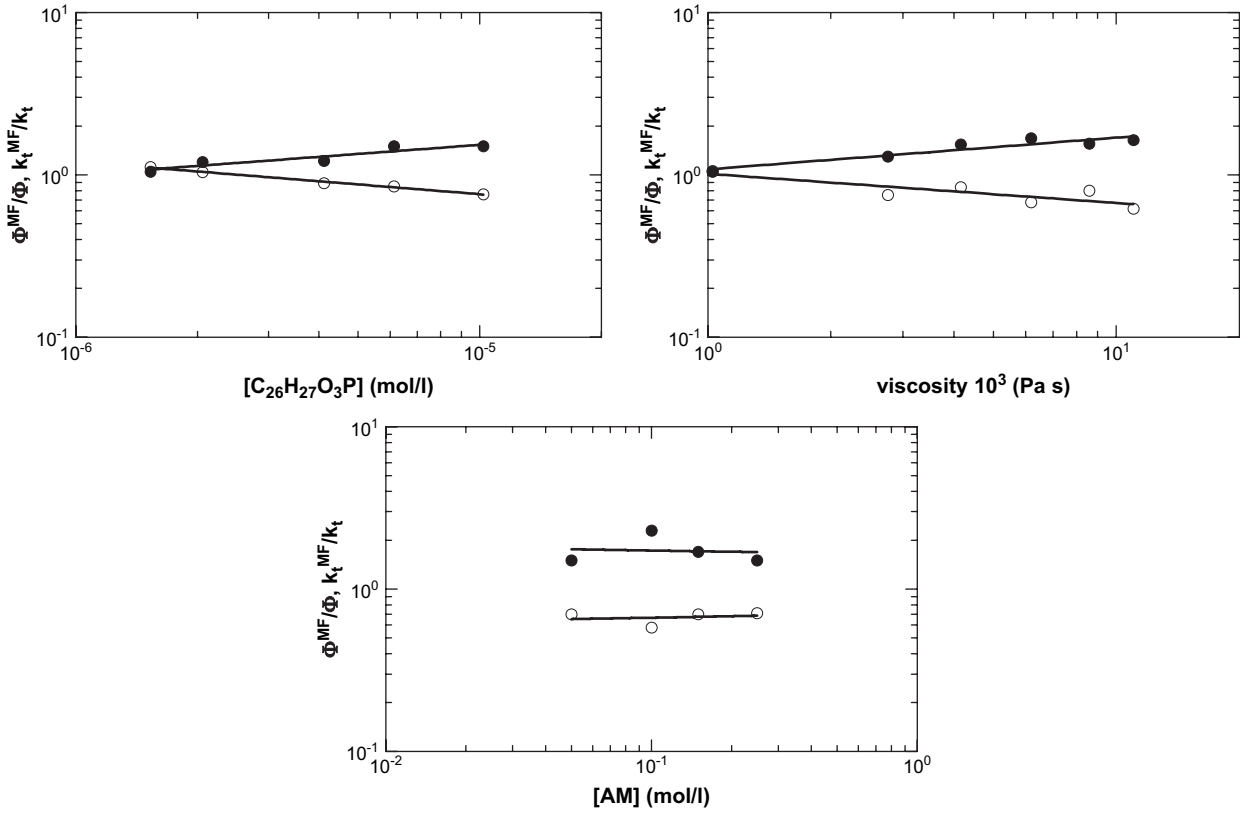

Fig. 12. The ratios Φ^{MF}/Φ (●) and k_t^{MF}/k_t (○) as functions of the initiator concentration, viscosity, and monomer concentration (the linearity of the logarithmic plots suggests leveling off of the effects of the initiator concentration and the viscosity).

The influence of the MF on Φ and k_t is explicitly visible from the ratios Φ^{MF}/Φ and k_t^{MF}/k_t presented in Fig. 12, since all the other reaction conditions were kept constant for this comparison of identical polymerizations without and with MF. Consequently, neither monomer concentration, initiator concentration, viscosity, or temperature has to be considered as an influence on k_t, while comparing only two polymerizations. In addition, the change of the ratios with [AM], [$C_{26}H_{27}O_3P$], and viscosity becomes graphically visible. The invariability of k_p with MF will be demonstrated in Section 4.1.

4. Discussion

The absence of polymerization in series 1 and 2 proves that the generation of free radicals via monomer or solvent photolysis (series 1) and thermal decomposition of $C_{26}H_{27}O_3P$ (series 2), which could initiate undesired polymerization, are insignificant. Consequently, these two sources of radical generation can be neglected in further analysis. The results of series 1 and 2 are of particular importance since the equations in the theoretical part were developed assuming that polymerization reactions are initiated only by photochemical dissociation of $C_{26}H_{27}O_3P$.

4.1. Absence of MF effect on the propagation step and monomer exponent

MF effects associated to spin quenching in T_+ state are not expected for initiation and termination steps in thermal polymerizations since radical pairs are generated and terminated in the S state, which may pass to the T_0 state and vice versa. Neither, the original spin state nor the probability of recombination, transformation in cage products, and escape of the radicals are affected by an external MF of 0.1 T [9]. Moreover, MF effects associated with spin quenching in T_+ state require the interaction between two radicals, which is certainly not the case of a propagation step where only one radical at the polymer chain end participates in the reaction. However, favorable molecular orientation of growing radicals and monomer molecules may facilitate the propagation reaction. Thus, higher R_p, as the consequence of a magnetically induced increment of k_p due to molecular orientation, cannot be excluded a priori. Conversely, the identical polymerization paths for thermal polymerizations of series 3 (Fig. 5) prove that the MF orientation of monomers and growing radicals, and, consequently, its effects on k_p, are insignificant in the limits of the experimental conditions applied here. As the propagation step can be considered as independent of the routes of initiation and termination, invariability of k_p with MF may be suggested to be valid also in photochemically initiated polymerizations.

The monomer exponents, $\alpha = 1.01$ and $\alpha^{MF} = 1.12$, determined by linear regressions in Fig. 8, differ by 10%. This can be considered as within the experimental error since α, in general, was reported in the range between 1.00 [26,27] and 1.16 [31]. Neither the presence of EG in the polymerization media nor the application of MF could considerably deviate the first order dependency of R_p on [M]. Such result

validates the assumption of $\alpha = 1$ in Eq. (3). Consequently, it can be concluded that k_p and α were not affected by 0.1 T of MF intensity in thermally as well as in photochemically initiated polymerizations.

On the other hand, it is well known that k_p of acrylamide strongly depends on the monomer concentration, in particular in the range $0.3 < [AM] < 1.5$ mol/l [25]. A variety of reasons were discussed for the change of k_p with the monomer concentration [22,25,37–40]. The AM concentration of the present study was selected below this well studied monomer concentration range. Therefore, the influence of [AM] on k_p at this low concentration can only be speculated due to the lack of reliable data. It is not clear if k_p further increases when [AM] decreases exceeding the values reported in Ref. [25], or if k_p levels off. The first may be suggested from the data in Table 3 as the reason for $k_p/k_t^{0.5}$ and $(k_p/k_t^{0.5})^{MF}$ decreasing with increasing [AM].

4.2. Absence of MF effects on the molar absorptivity

The value of the molar absorptivity at $\lambda = 254$ nm in Fig. 10, $\varepsilon = 6700$ l/mol cm, is about 18% lower than the average of the values obtained by the dead-end technique shown in Table 3, $\varepsilon = 7914 \pm 1260$ l/mol cm, though it is within the range of the standard deviation σ. This proves the principal suitability of the dead-end technique to determine the molar absorptivity indirectly using kinetic data. The advantage is the in situ determination under real polymerization conditions. Table 3 also reveals that ε was affected neither by $[C_{26}H_{27}O_3P]$, η, [AM], nor by MF.

4.3. MF effects on the initiator efficiency

The initiator exponent, β, was altered from 0.10 to 0.28 for polymerizations without and with MF (Fig. 6), respectively. However, deviations from the square root dependency do not conclusively indicate modifications in the mechanisms of radical generation and termination. They are always generated and terminated in pairs. Therefore, $\beta = 0.5$, as it was assumed in Section 2.5, may be considered as valid. More appropriately, the apparent deviations of β from its ideal value may be caused by variation of Φ with the initiator concentration [11]. Consequently, it was considered here that Φ is actually a function of $[C_{26}H_{27}O_3P]$, η, [AM], and MF, too.

Results of series 4 show that $C_{26}H_{27}O_3P$ is less efficient at high initiator concentration, probably due to radical transfer to the initiator. The decomposition of initiator due to radical transfer reactions does not change the radical concentration during the polymerization since the newly formed radical will initiate a new polymer chain. However, the reaction does result in wastage of initiator. Such reaction is more probable at high than at low initiator concentration.

Results of series 5 indicate that $C_{26}H_{27}O_3P$ is more efficient at high η. The formation of cage products implies rotations and displacements of caged radicals. High viscosity media impair such molecular movements and, therefore, the formation of cage products. Though, as the radical pair remains trapped in the cage, the recombination reaction is by far the most probable reaction.

Results of series 6 show that the initiator is more efficient at high monomer concentration. At their instant of formation, the primary radicals are trapped in a cage formed by solvent and monomer molecules. The reaction between a primary radical with a cage forming monomer molecule yields the radical outside of the cage, which initiates the propagation process. Therefore, an increment in the number of monomer molecules forming the cage would increase the probability of reaction between a monomer molecule, with a primary radical facilitating the escape from the cage and reducing the formation of cage products.

The application of MF increases Φ. This is demonstrated by $\Phi^{MF}/\Phi > 1$ in the plots of Fig. 12. It occurs by quenching the radicals in the T_+ state according to the radical pair mechanism for intersystem crossing of spin states. The radical pair in T_+ state is inhibited to undergo recombination and formation of cage products. It has more chances to initiate the propagation reaction. At high initiator concentration, where the initiator efficiency is very low, the MF effect seems to be more evident. It can be concluded that the MF effect is small in comparison with the changes induced by radical transfer to the initiator.

High viscosity media enhance the MF effect. Here, the spin quenching effect due to the application of MF is added to the molecular immobilization effect. Both effects extend the lifetime of the radicals trapped in the cage. This increases the probability to react with a cage forming monomer molecule and, thus, to escape from the cage. Spin quenching inhibits in the same manner recombination and cage product reactions, while high viscosity media inhibit only the molecular movements involved in the formation of cage products.

4.4. MF effects on the termination reaction

The increment of the $k_p/k_t^{0.5}$ ratio with $[C_{26}H_{27}O_3P]$ is obviously caused by a decrease of k_t since k_p can be considered unaffected by the initiation process. In fact, the ratio $k_p/k_t^{0.5}$ was obtained at steady state conditions where initiation and termination rates are equal, which allows expressing k_t as

$$k_t = \frac{\Phi \varepsilon I_0 [I]}{[M^\bullet]^2} \tag{7}$$

Here it is visible that k_t depends directly on [I] and inversely on the square concentration of growing radials, $[M^\bullet]^2$. However, it must be noted that an increment in [I] would also increase $[M^\bullet]$. This may cause a sharp decrease of k_t due to its square dependency on $[M^\bullet]$. An increment of η certainly would decrease k_p and k_t due to the reduction of the mobility of growing radicals and monomers. However, the decrease of k_t is expected to be much more pronounced than a decrease of k_p due to the different mobility of growing radicals and monomer molecules. Such a difference in the decrease of k_p and k_t may explain the increment of the $k_p/k_t^{0.5}$ ratio with η. Finally,

the decrease of the $k_p/k_t^{0.5}$ ratio with [M] becomes obvious when analyzing Eq. (1).

It was demonstrated in Section 4.1 that k_p is unaffected by MF and, consequently, it cancels out during the calculation of the k_t^{MF}/k_t ratio. The k_t^{MF}/k_t ratios obtained are presented in Fig. 12. k_t^{MF}/k_t tends to decrease with increasing [$C_{26}H_{27}O_3P$] and η, though is unaffected by [AM]. The effects are evidently caused by decrease of k_t^{MF} when MF was applied. Here, the $T_+ \rightarrow S$ relaxation time seems to be longer than the classical lifetime of the radicals. In such a case, when two radicals encounter each other, they present a T_+ state that is unable to undergo termination reactions resulting in a decrease of k_t.

4.5. MF effects on the molar mass

It was not the purpose of this work to perform extended polymer characterization. [η] was determined as an estimate. The variation of [η] for polymers obtained without and with MF under otherwise identical conditions was within the experimental error. Therefore, no influence of the MF on the molar mass was concluded for the system and conditions studied here.

At first sight, this is somehow surprising due to the clearly proved increase of the initiator efficiency when MF was applied. Higher initiator efficiency should decrease the molar mass. Compensation of this effect by the simultaneously decreasing k_t is suggested as explanation. Controversial reports by several authors may result from situations where the increase of Φ and decrease of k_t did not match and balance each other. Depending on the situation, if the increase of Φ, or the decrease of k_t, with MF dominates the kinetics, lower or higher molar masses can be expected with MF. Such an example is the polymerization of acrylic acid in the MF, for which an increase of the molar mass was found, in particular at high pH. These results will be the subject of a separate publication [41].

5. Conclusions

MF inhibits recombination of initial radicals, formation of cage products, and termination reactions between growing radicals in photochemically initiated polymerizations. The effect is enhanced in high viscous medium and at high initiator and monomer concentrations. This results in significant increments of Φ and β but decrease of k_t with MF. Contrarily, thermally initiated polymerizations are not affected by MF. The radical pair mechanism for intersystem crossing of spin states explains MF effects on Φ, β, and k_t. Slight variations of the MF intensity are suggested to maximize or minimize the initiator efficiency and the termination rate coefficient, respectively.

k_p, α, and ε can be considered as unaffected by 0.1 T of MF intensity. This indicates that orientation of monomer molecules and structural changes of the initiator are negligible at such MF strength. However, MF effects on these parameters may become significant at higher MF. Specifically, the 10% difference between α^{MF} and α may indicate some degree of magnetic orientation of monomer molecules. This has to be proved.

Of practical interest can be that the application of low intensity MF increases R_p of the radical solution polymerization of acrylamide without decreasing the molar mass. Thus the R_p increment, which may directly be related to a reduction of residence times and productivity increase, can be achieved without altering recipe formulation, temperature profiles, and other reaction conditions.

Acknowledgements

The authors thank the Swiss National Science Foundation for the financial support (grants 2000-63395 and 200020-100250), Ciba Specialties for providing the photoinitiator as Irgacure 819DW, and Dr. Giovanni Boero from the Laboratory of MicroSystems of the EPFL for assistance with the electromagnet.

References

[1] Salikhov KM, Molin YN, Sagdeev RZ, Bucharenko AL. In: Molin YN, editor. Spin polarization and magnetic effects in radical reactions. Amsterdam: Elsevier; 1984 [chapter 1].
[2] Maiti S, Bag DS. J Polym Mater 1993;10:287–93.
[3] Huang JL, Song QH. Macromolecules 1993;26(6):1359–62.
[4] Bag DS, Maiti S. Polymer 1998;39(3):525–31.
[5] Simionescu CI, Chiriac AP, Neamtu I. Polym Bull 1991;27(1):31–6.
[6] Bag DS, Maiti S. J Polym Sci Part A Polym Chem 1998;36(10):1509–13.
[7] Simionescu CI, Chiriac AP. Colloid Polym Sci 1992;270(8):753–8.
[8] Vedeneev AA, Khudyakov IV, Golubkova NA, Kuzmin VA. J Chem Soc Faraday Trans 1990;86(21):3545–9.
[9] Steiner UE, Ulrich T. Chem Rev 1989;89(1):51–147.
[10] Khudyakov IV, Arsu N, Jockusch S, Turro NJ. Des Monomers Polym 2003;6(1):91–101.
[11] Odian G. Principles of polymerization. 4th ed. New Jersey: Wiley-Interscience; 2004 [chapter 3].
[12] Kolczak U, Rist G, Dietliker K, Wirz J. J Am Chem Soc 1996;118(27):6477–89.
[13] Sartomer C. A study of initiating systems for photopolymerization. www.sartomer.com.
[14] Australian National Industrial Chemicals Notification and Assessment Scheme. GPO Box 58, Sydney 2001, Australia.
[15] Ghosh P, Pal G. Eur Polym J 1997;33(10–12):1695–700.
[16] Liu LY, Yang WT. J Polym Sci Part A Polym Chem 2004;42(4):846–52.
[17] Alric J, David G, Boutevin B, Rousseau A, Robin JJ. Polym Int 2002;51(2):140–9.
[18] Tripathi S, Srivastava AK. J Polym Sci Part A Polym Chem 2004;42(9):2060–5.
[19] Cabaness WR, Lin TYC, Parkanyi C. J Polym Sci Part A-1 Polym Chem 1971;9(8):2155–70.
[20] Currie DJ, Daiton FS, Watt WS. Polymer 1965;6(9):451–3.
[21] Pascal P, Napper DH, Gilbert RG. Macromolecules 1990;23(24):5161–3.
[22] Pascal P, Winnik MA, Napper DH, Gilbert RG. Macromolecules 1993;26(17):4572–6.
[23] Gromov VF, Galperina NI, Osmanov TO, Khomikovski PM, Abkin AD. Eur Polym J 1980;16(6):529–35.
[24] Hunkeler D. Macromolecules 1991;24(9):2160–71.
[25] Seabrook SA, Tonge MP, Gilbert RG. J Polym Sci Part A Polym Chem 2005;43(7):1357–68.

[26] Baade W, Reichert KH. Eur Polym J 1984;20(5):505–12.
[27] Collinson E, Dainton FS, McNaughton GS. Trans Faraday Soc 1957; 53(4):476–88.
[28] Cavell EAS. Makromol Chem 1962;54:70–7.
[29] Riggs JP, Rodrigues F. J Polym Sci Part A-1 Polym Chem 1967;5(12): 3167–81.
[30] Candau F, Leong YS, Fitch RM. J Polym Sci Part A Polym Chem 1985; 23(1):193–214.
[31] Fanood MHR, George MH. Polymer 1988;29(1):128–33.
[32] Rintoul I, Wandrey C. Polymer 2005;46(13):4525–32.
[33] Tobolsky AV, Rodgers CE, Brickman RD. J Am Chem Soc 1960;82(6): 1277–80.
[34] Bohme RD, Tobolsky AV. Dead-end polymerization. In: Encyclopedia of polymer science and technology, vol. 4. New York: John Wiley & Sons, Inc.; 1966. p. 599–605.
[35] Gobran RH, Berenbaum MB, Tobolsky AV. J Polym Sci 1960;46(148): 431–40.
[36] Misra GS, Bhattacharya SN. Eur Polym J 1979;15(2):125–8.
[37] Lacik I, Beuermann S, Buback M. Macromolecules 2001;34(18):6224–8.
[38] Ganachaud F, Balic R, Monteiro MJ, Gilbert RG. Macromolecules 2000; 33(23):8589–96.
[39] Thickett S, Gilbert RG. Polymer 2004;45(20):6993–9.
[40] Tanaka N, Kitano H, Ise N. J Phys Chem 1990;94(16):6290–2.
[41] Rintoul I. Ph.D. Thesis, No. 3444. EPFL; 2006.